Performance Assessment of Data Sampling Strategies for Neural Network-based Voltage Approximations

Richard Asiamah, Rahul K. Gupta, Rabab Haider, and Daniel K. Molzahn
School of Electrical and Computer Engineering, Georgia Institute of Technology, Atlanta, USA
{asiamah, rahul.gupta, rabab.haider, molzahn}@gatech.edu

***Abstract*—Machine learning models have been developed for a wide variety of power system applications. The accuracy of a machine learning model strongly depends on the selection of training data. In many settings where real data are limited or unavailable, machine learning models are trained using synthetic data sampled via different strategies. Using the task of approximating the voltage magnitudes associated with specified complex power injections as an illustrative application, this paper compares the performance of neural networks trained on four different sampling strategies: (i) correlated loads at fixed power factor, (ii) correlated loads at varying power factor, (iii) uncorrelated loads at fixed power factor, and (iv) uncorrelated loads at varying power factor. A new sampling strategy that combines these four strategies into one training dataset is also introduced and assessed. Results from transmission and distribution test cases of varying sizes show that these strategies for creating synthetic training data yield varied neural network accuracy. The accuracy differences across the various strategies vary by up to a factor of four. While none of the first four strategies outperform the others across all test cases, neural networks trained with the combined dataset perform the best overall, maintaining a high accuracy and low error spreads.**

***Index Terms*—Neural Network, Power Flow, Sampling.**

I. Introduction

Recently, the application of Machine Learning (ML) methods to power systems physics has gained significant attention. These methods can address the inherent non-linearity of power systems and reduce computational complexity through application-specific training. These applications are surveyed in [1]–[3] and include power flow analysis [4], state estimation [5], [6], optimal power flow [4], [7], voltage control [8], and topology reconfiguration [9], [10], among others.

Neural Network (NN)-based methods have received notable interest, especially in solving the power flow equations. These methods mitigate the online computational burden associated with AC power flow analysis by employing models trained offline. NN methods utilize training data to infer the power flow relationships. The selected training data greatly influences the model's ability to predict unseen conditions accurately. Many references, such as [11]–[14], suggest using previous/historical data when training neural networks. While using historical data from measurements eliminates the need for an explicit power system model, sufficient historical data may not always be available to train a neural network effectively due to limited sensor availability and data confidentiality. Moreover, historical data may not necessarily represent future system operations, especially during extreme events or contingencies. Thus, it is often necessary to generate synthetic training data.

Different strategies have been used in literature to generate synthetic training data. For example, [10], [15]–[19] use independent Gaussian sampling, while [20], [21] use spatially correlated sampling. The biggest argument for the latter is that real-time load variations are often driven by common factors (e.g., a common ambient temperature across a region strongly influences air conditioner load), making correlated sampling appropriate. At the same time, the former could improve the generalizability to wider ranges of power injection variability.

To better understand the implications of various sampling strategies for generating training data, this paper characterizes how different data sampling choices affect neural network accuracy. Using a fully connected neural network for approximating voltage magnitudes as an illustrative application, we compare four sampling strategies: (i) correlated load demands at fixed power factor, (ii) correlated load demands at varying power factor, (iii) uncorrelated load demands at fixed power factor, and (iv) uncorrelated load demands at varying power factor. We evaluate the performance of neural networks trained with each strategy for unseen test data that may be correlated or uncorrelated and exhibit either a constant or varying power factor. We also evaluate their performance for different loading conditions, including actual time-series measurements. Thus, this paper's key contribution is a detailed performance assessment of a simple NN model's voltage approximation accuracy with respect to different training data sampling strategies considering comparisons across different loading conditions.

The paper is organized as follows. Section II presents notation, background regarding the power flow equations, and a neural network model for predicting voltage magnitudes. Section III presents different strategies for synthetic training data generation. Section IV presents our numerical results and key findings. Section V concludes the paper.

II. Background

We first present notation and background material regarding the power flow equations and the neural network model we

Support from NSF award #2145564 is gratefully acknowledged.

use as an illustrative application.

A. AC power flow model

Consider an n-bus power system with sets of buses $\mathcal{B}$ and branches $\mathcal{L}$. Each bus $i \in \mathcal{B}$ has active and reactive power injections P_i and Q_i and voltage magnitude and angle, V_i and θ_i. The vector of active and reactive load demands at all buses is denoted as $\mathbf{P}_D$ and $\mathbf{Q}_D$. The network admittance matrix is $\mathbf{Y} = \mathbf{G} + j\mathbf{B}$, where $j = \sqrt{-1}$. Define $\theta_{ik} = \theta_i - \theta_k$ for all branches $(i,k) \in \mathcal{L}$. Given these definitions, the AC power flow equations relating the power injections and voltage phasors are:

$$P_i = V_i \sum_{k=1}^{n} V_k \left(\mathbf{G}_{ik}\cos(\theta_{ik}) + \mathbf{B}_{ik}\sin(\theta_{ik})\right), \tag{1a}$$

$$Q_i = V_i \sum_{k=1}^{n} V_k \left(\mathbf{G}_{ik}\sin(\theta_{ik}) - \mathbf{B}_{ik}\cos(\theta_{ik})\right). \tag{1b}$$

The AC power flow equations (1) are usually solved by numerical methods such as Newton-Raphson to obtain the grid states, i.e., the voltage magnitudes and angles. However, such computations are computationally demanding if they need to be carried out multiple times (e.g., for Monte Carlo simulations). ML models have recently been proposed to address this challenge, e.g., [22], [23]. Next, we describe one such model that uses a neural network architecture.

B. NN-based Voltage Prediction Model

Given the AC power flow equations (1), we focus on the task of approximating the voltage magnitudes given the buses' active and reactive power injections. To do so, we use a simple, fully connected neural network with one hidden layer of ReLU activation functions. Fig. 1 shows the architecture, where the inputs to the network are vectors of the real and reactive power injections and the output is the vector of approximated voltage magnitudes, denoted as $\hat{\mathbf{V}}$. The system determines the size of the input and output layers: the input layer has size $2 \times |\mathcal{B}|$ corresponding to the active and reactive power injections at every bus, and the output layer has size $|\mathcal{B}|$ corresponding to the voltages approximated at every bus. The size of the hidden layer (number of neurons) is determined by hyperparameter tuning and is set at 100 neurons for all experiments in this paper. Using training data sampled according to the strategies discussed in Section III, we train neural networks to approximate the nonlinear AC power flow equations using the Adam optimizer set at a learning rate of 0.001 [24]. The loss function sums, across all samples, the Mean Absolute Error (MAE) in the voltage approximations across all buses:

$$\text{MAE} = \frac{\sum_{i\in\mathcal{B}} |\hat{V}_i - V_i|}{|\mathcal{B}|}. \tag{2}$$

The datasets are split into 80% training and 20% testing. An early stopping criterion is used to prevent overfitting to the training set, using a patience value of ten epochs.

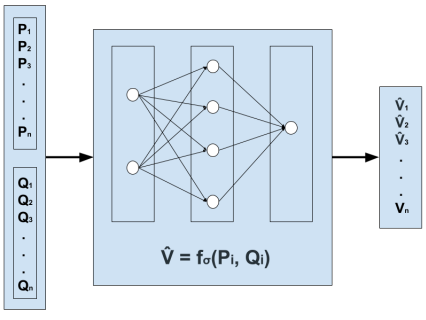

Fig. 1: A simple neural network with one hidden layer. The network is trained to approximate the voltage magnitudes based on the power injections at each bus.

III. Synthetic dataset creation

This paper's key contribution is a comparative analysis of different strategies to generate synthetic datasets for voltage prediction using the NN model described in Section II. To sample the power injections, we vary the load demand at every bus while keeping the generator outputs at all buses fixed, except for the slack bus, which balances power as needed to satisfy the power flow equations. We consider five strategies:

(i) **Correlated load, same power factor (CS)**: All loads are assumed to be perfectly correlated. To generate a wide range of the data for different loading conditions, we multiply all the load demands by a common factor $\alpha \in \mathbb{R}$ sampled from a $\pm 50\%$ uniform distribution $\alpha \sim \mathcal{U}(0.5, 1.5)$, i.e., the new load data point is calculated as $\mathbf{P}_D = \alpha \mathbf{P}_D^*$, where $\mathbf{P}_D^*$ denotes the nominal active power load. For the reactive power, we assume a *constant power factor*, i.e., the reactive loads are obtained by multiplying the nominal reactive power demand $\mathbf{Q}_D^*$ by the same value of α, that is, $\mathbf{Q}_D = \alpha \mathbf{Q}_D^*$.

(ii) **Correlated load, varying power factor (CV)**: The active loads are modified in the same manner as in CS, but the reactive power is sampled independently of the active power. This is done by sampling a *new value* of the multiplying factor, $\alpha_Q \in \mathbb{R}$, from the $\pm 50\%$ uniform distribution $\alpha_Q \sim \mathcal{U}(0.5, 1.5)$ and applying this factor as $\mathbf{Q}_{,D} = \alpha_Q \mathbf{Q}_D^*$.

(iii) **Uncorrelated load, same power factor (US)**: The active loads are multiplied by unique multiplicative factors, $\boldsymbol{\alpha} \in \mathbb{R}^{|\mathcal{B}|}$. Each load P_{Di}, $\forall i \in \mathcal{B}$, is perturbed from the corresponding nominal load as $P_{Di} = \alpha_i P_{Di}^*$. The reactive power is created similarly to CS, i.e., with a constant power factor, that is, $Q_{Di} = \alpha_i Q_{Di}^*$.

(iv) **Uncorrelated load, varying power factor (UV)**: All the active and reactive loads are uncorrelated and are obtained by multiplying with separate factors, α_i and α_{Qi}, sampled from the $\pm 50\%$ uniform distribution, i.e., α_i, $\alpha_{Qi} \sim \mathcal{U}(0.5, 1.5)$. Thus, for all $i \in \mathcal{B}$, $P_{Di} = \alpha_i P_{Di}^*$ and $Q_{Di} = \alpha_{Qi} Q_{Di}^*$.

(v) **Combined Dataset**: This dataset combines the different strategies in *equal proportion*. We equally combine strategies (i)–(iv) to generate a new dataset that encompasses

all load variations, i.e., correlated versus uncorrelated load, as well as varying and constant power factors. For example, a dataset of 100 data points contains 25 instances of (i), 25 instances of (ii), etc.

We also consider three loading levels for each dataset to represent the demand variation observed in electricity grids:

- **Nominal loading**: Active and reactive loads are varied between 95% and 105% of the nominal value.
- **Overloading**: Active and reactive loads are varied between 130% and 150% of the nominal value.
- **Underloading**: Active and reactive loads are varied between 50% and 70% of the nominal value.
- **Time-series**: We also test the trained models using time series data obtained from real grid measurements using the setup described in [25].

Notably, the overloading and underloading datasets present unusual loading conditions that may be underrepresented in historical data but are becoming increasingly common in the advent of extreme weather conditions [26]. Their uncommon nature makes them more challenging to manage [27], [28].

IV. Numerical Results

This section presents a performance comparison of the training data sampling strategies described in Section III for voltage magnitude prediction using the NN model reviewed in Section II. The neural network accuracies achieved with different training data strategies are evaluated based on the Percentage of In-Tolerance Predictions (PTol):

$$\text{PTol}(\epsilon) = \frac{\sum_{j\in \mathrm{T}} \sum_{i\in\mathcal{B}} \mathbb{I}(|\hat{\mathbf{V}}_j - \mathbf{V}_j| < \epsilon)}{|\mathcal{B}| \times \mathrm{T}} \times 100\%, \qquad (3)$$

where $\hat{\mathbf{V}}$ is the vector of approximated voltage magnitudes, $\mathbf{V}$ is the vector of actual voltage magnitudes obtained from computing the power flow, $\mathbb{I}$ denotes the indicator function, T is the size of the testing dataset, and ϵ indicates the tolerance level for the PTol metric. The ϵ value is given in per unit (pu). Higher values of PTol indicate better accuracy since a larger percentage of predictions are within the specified tolerance. Additionally, higher PTol values for smaller tolerance levels ϵ also indicate better accuracy.

A. Test-case and implementation

We perform numerical tests using five networks of varying sizes: the IEEE 14-bus and 118-bus test systems, a radial 33-bus distribution grid [29], and two models representative of real grids: the Swedish 503-bus system [30] and the European 906-bus system [31].

We vary the active and reactive power demands via the five strategies described in Section III. Using the Julia programming language [32], the power flow problems were solved using the PowerModels [33] package with the nonlinear solver IPOPT [34]. The neural network training was conducted using the Flux package [35] on a computer with an 8-core Mac-M2 chip at 3.2GHz and 16 GB of RAM.

B. Results from Testing Datasets

For each sampling strategy and the same neural network structure, the neural networks' accuracies in predicting nodal voltages are adjudged by comparing the approximated voltages to the actual voltage magnitude values obtained by solving the AC power flow equations (1). We assess the ability of the different strategies to approximate voltage magnitudes within acceptable tolerance levels for nominal, overloaded, and underloaded conditions. For each sampling method, we show the PTol values for the specified ϵ values over $\mathrm{T} = 250$ testing samples. We evaluate the accuracy of the NN when trained using the different sampling strategies by testing on validation datasets generated using other strategies under each range of loading conditions. Fig. 2 details the results of this evaluation.

The results show that the combined dataset performs the best overall. While none of the first four strategies maintained consistency in the results in all the test cases, the combined dataset displays a much more undeviating pattern. For all the test cases, NNs trained with the combined dataset maintained a consistently good performance by reaching a PTol value of 100% with the ϵ value set at 0.01 pu.

The same cannot be said for any of the first four methods. For instance, the UV and US sampling strategies performed best for the IEEE 14-bus system, with all approximated voltages within 0.001 pu of the actual values. However, these strategies perform poorly for the Swedish 503-bus and European 906-bus test cases, especially under extreme loading conditions. Conversely, CS and CV show the best performance for the Swedish 503-bus test case, but they are the worst-performing strategies for the IEEE 14-bus and radial 33-bus test cases.

The combined dataset, on the other hand, is consistent in providing good accuracy. The combined dataset performs at least as well as, if not better, than any of the first four strategies for all loading conditions. The combined strategy performs just as well as CS and CV strategies for the IEEE 118-bus case and equally as well as US and UV strategies for the IEEE 14-bus and radial 33-bus cases. This indicates a consistency in the positive results obtained from the combined dataset.

C. Comparison using Time-Series Data

To further assess the performance abilities of the different data generation methods, we test the accuracy of the various sampling strategies on the real-time-series data from [25]. For a 24-hour period, we make predictions of the voltage magnitudes at every bus and compute the absolute value of the approximation error. The error spread for each method in the various test networks is shown in Fig. 3.

For all the networks, the combined dataset produced the best results with the smallest spread of errors and, in most cases, had the average error closest to zero. Again, similar to results in Fig. 2, none of the four commonly used strategies demonstrated consistency in the prediction results. UV and US performed very well for the smaller test cases but significantly underperformed for the larger test cases. Similarly, while

TESTED WITH	UNDERLOADING					NOMINAL LOADING					OVERLOADING					
	CS	CV	US	UV	Combined	CS	CV	US	UV	Combined	CS	CV	US	UV	Combined	
CS	18.68	38.74	100.00	99.66	30.95	23.08	38.46	100.00	100.00	30.77	15.42	24.52	17.51	49.82	22.80	ε = 0.001
CV	12.46	40.25	59.51	99.97	31.08	22.40	41.23	88.00	100.00	30.77	17.85	25.45	8.55	49.26	23.94	
US	13.54	16.55	100.00	100.00	31.66	21.45	32.25	100.00	100.00	27.69	16.62	20.77	1.11	50.49	24.40	
UV	10.49	16.98	36.77	100.00	28.83	20.18	33.51	78.25	100.00	27.51	12.31	18.77	1.51	50.58	22.89	
Combined	13.08	28.55	74.15	99.94	30.49	21.66	37.17	91.88	100.00	29.32	15.72	22.89	6.83	49.91	23.23	
CS	18.68	38.74	100.00	99.66	30.95	23.08	38.46	100.00	100.00	30.77	15.42	24.52	17.51	49.82	22.80	ε = 0.002
CV	12.46	40.25	59.51	99.97	31.08	22.40	41.23	88.00	100.00	30.77	17.85	25.45	8.55	49.26	23.94	
US	13.54	16.55	100.00	100.00	31.66	21.45	32.25	100.00	100.00	27.69	16.62	20.77	1.11	50.49	24.40	
UV	10.49	16.98	36.77	100.00	28.83	20.18	33.51	78.25	100.00	27.51	12.31	18.77	1.51	50.58	22.89	
Combined	13.08	28.55	74.15	99.94	30.49	21.66	37.17	91.88	100.00	29.32	15.72	22.89	6.83	49.91	23.23	
CS	68.77	76.92	100.00	100.00	68.43	61.54	76.92	100.00	100.00	61.54	56.77	66.71	27.57	98.03	48.71	ε = 0.005
CV	33.23	76.92	85.38	100.00	67.78	58.55	76.92	99.26	100.00	61.54	41.08	69.38	17.88	99.23	49.08	
US	33.35	40.37	100.00	100.00	71.51	54.65	66.86	100.00	100.00	62.31	41.48	46.74	4.28	99.78	55.26	
UV	25.69	39.82	73.51	100.00	68.55	52.74	68.12	99.38	100.00	64.06	31.32	46.18	6.40	99.94	56.62	
Combined	38.83	58.68	89.45	100.00	67.82	57.17	72.68	99.69	100.00	62.68	42.80	57.78	15.32	99.11	51.32	
CS	100.00	100.00	100.00	100.00	100.00	100.00	100.00	100.00	100.00	100.00	99.94	95.38	40.65	100.00	98.22	ε = 0.01
CV	61.42	100.00	96.86	100.00	100.00	91.97	100.00	100.00	100.00	100.00	70.18	98.25	36.31	100.00	99.63	
US	61.26	69.20	100.00	100.00	99.05	93.38	94.46	100.00	100.00	100.00	71.97	77.20	31.51	100.00	96.80	
UV	48.25	69.60	95.29	100.00	96.62	87.63	94.98	100.00	100.00	100.00	59.26	76.58	33.32	100.00	93.78	
Combined	66.40	84.77	98.03	100.00	98.98	93.00	97.26	100.00	100.00	100.00	75.48	87.72	35.78	100.00	97.32	

(a) IEEE 14-bus system

TESTED WITH	UNDERLOADING					NOMINAL LOADING					OVERLOADING					
	CS	CV	US	UV	Combined	CS	CV	US	UV	Combined	CS	CV	US	UV	Combined	
CS	84.76	60.30	100.00	99.75	89.18	84.38	89.91	100.00	100.00	88.06	58.78	31.64	29.11	59.21	75.58	ε = 0.001
CV	79.73	57.96	96.13	99.96	89.13	84.73	90.21	100.00	100.00	87.80	58.24	31.62	26.97	57.35	76.88	
US	62.05	43.54	100.00	100.00	80.79	81.91	87.29	100.00	100.00	87.40	54.64	29.81	26.70	56.78	73.88	
UV	65.08	43.64	97.14	100.00	80.71	82.41	88.35	100.00	100.00	87.51	54.70	30.46	27.34	56.61	74.80	
Combined	72.71	51.75	98.08	99.95	85.06	83.50	88.89	100.00	100.00	87.64	55.64	30.81	27.31	57.03	75.30	
CS	84.76	60.30	100.00	99.75	89.18	84.38	89.91	100.00	100.00	88.06	58.78	31.64	29.11	59.21	75.58	ε = 0.002
CV	79.73	57.96	96.13	99.96	89.13	84.73	90.21	100.00	100.00	87.80	58.24	31.62	26.97	57.35	76.88	
US	62.05	43.54	100.00	100.00	80.79	81.91	87.29	100.00	100.00	87.40	54.64	29.81	26.70	56.78	73.88	
UV	65.08	43.64	97.14	100.00	80.71	82.41	88.35	100.00	100.00	87.51	54.70	30.46	27.34	56.61	74.80	
Combined	72.71	51.75	98.08	99.95	85.06	83.50	88.89	100.00	100.00	87.64	55.64	30.81	27.31	57.03	75.30	
CS	96.88	87.09	100.00	100.00	100.00	96.88	100.00	100.00	100.00	100.00	93.76	51.51	50.91	98.96	99.94	ε = 0.005
CV	95.86	89.96	100.00	100.00	100.00	96.86	100.00	100.00	100.00	100.00	93.05	52.25	48.31	99.46	99.99	
US	94.39	83.53	100.00	100.00	99.99	96.75	99.43	100.00	100.00	100.00	91.30	51.96	41.84	99.96	99.93	
UV	94.96	84.05	100.00	100.00	99.98	96.74	99.45	100.00	100.00	100.00	91.94	51.34	42.06	100.00	99.86	
Combined	95.30	86.45	100.00	100.00	100.00	96.83	99.71	100.00	100.00	100.00	92.43	51.28	45.71	99.51	99.95	
CS	100.00	97.91	100.00	100.00	100.00	100.00	100.00	100.00	100.00	100.00	99.52	81.94	85.43	100.00	100.00	ε = 0.01
CV	100.00	98.78	100.00	100.00	100.00	100.00	100.00	100.00	100.00	100.00	99.85	81.99	88.52	100.00	100.00	
US	99.74	99.85	100.00	100.00	100.00	100.00	100.00	100.00	100.00	100.00	99.56	81.65	93.84	100.00	100.00	
UV	99.86	99.85	100.00	100.00	100.00	100.00	100.00	100.00	100.00	100.00	99.74	81.63	93.56	100.00	100.00	
Combined	99.90	98.99	100.00	100.00	100.00	100.00	100.00	100.00	100.00	100.00	99.64	81.30	89.50	100.00	100.00	

(b) Radial 33-bus system

TESTED WITH	UNDERLOADING					NOMINAL LOADING					OVERLOADING					
	CS	CV	US	UV	Combined	CS	CV	US	UV	Combined	CS	CV	US	UV	Combined	
CS	18.97	0.01	25.99	1.59	16.00	18.10	0.00	12.07	9.56	12.67	13.79	1.73	0.00	0.00	0.19	ε = 0.001
CV	10.59	0.00	14.35	0.76	17.17	16.55	0.00	19.69	13.49	12.50	9.29	1.63	1.08	0.00	0.28	
US	4.29	3.34	16.50	0.00	11.66	11.00	1.30	0.00	0.06	14.71	5.08	3.06	0.00	0.00	2.38	
UV	4.19	3.59	11.51	0.00	10.15	11.26	1.20	22.77	0.00	15.03	5.46	3.23	1.07	0.00	2.83	
Combined	9.24	1.50	17.50	0.50	13.80	13.94	0.79	13.65	3.91	13.36	8.56	2.30	0.53	0.00	1.44	
CS	18.97	0.01	25.99	1.59	16.00	18.10	0.00	12.07	9.56	12.67	13.79	1.73	0.00	0.00	0.19	ε = 0.002
CV	10.59	0.00	14.35	0.76	17.17	16.55	0.00	19.69	13.49	12.50	9.29	1.63	1.08	0.00	0.28	
US	4.29	3.34	16.50	0.00	11.66	11.00	1.30	0.00	0.06	14.71	5.08	3.06	0.00	0.00	2.38	
UV	4.19	3.59	11.51	0.00	10.15	11.26	1.20	22.77	0.00	15.03	5.46	3.23	1.07	0.00	2.83	
Combined	9.24	1.50	17.50	0.50	13.80	13.94	0.79	13.65	3.91	13.36	8.56	2.30	0.53	0.00	1.44	
CS	48.05	0.18	58.67	3.16	50.84	42.30	0.00	66.17	26.27	37.69	25.62	4.45	0.02	0.00	2.79	ε = 0.005
CV	24.19	0.08	33.65	0.95	50.87	36.86	0.00	58.78	35.54	37.83	22.21	4.12	2.91	0.00	3.21	
US	11.23	8.43	60.64	0.00	28.55	26.57	3.33	99.90	18.36	38.04	13.01	7.65	0.00	0.00	6.15	
UV	10.99	8.65	28.55	0.00	25.34	27.72	3.21	56.02	16.43	38.11	13.44	8.04	2.76	0.00	7.58	
Combined	23.15	4.04	45.95	0.85	39.22	32.24	1.92	73.25	22.71	37.12	18.95	5.90	1.54	0.00	4.93	
CS	74.29	2.10	86.39	7.16	88.42	71.41	0.00	100.00	58.03	81.35	53.19	10.00	0.05	0.00	12.56	ε = 0.01
CV	44.03	2.09	59.50	1.20	89.20	63.10	0.00	92.93	68.53	80.54	39.81	9.00	7.48	0.00	13.40	
US	22.78	16.77	99.85	0.00	54.23	50.41	7.79	100.00	100.00	74.12	25.86	15.29	0.00	0.00	14.95	
UV	21.87	17.27	53.65	0.00	48.35	51.82	8.23	91.37	100.00	72.77	26.52	16.55	7.65	0.00	16.99	
Combined	40.15	8.93	74.76	2.25	70.50	58.09	4.41	96.75	82.76	76.84	36.98	12.43	3.95	0.00	14.34	

(c) IEEE 118-bus system

CS and CV perform well on the Sweden 503-bus system, this method underperforms on all other test cases, especially on the European 906-bus system, where the error spread is comparable to that of US and UV.

V. Conclusions

Recognizing that the accuracy of machine learning models strongly depends on the training data, this paper has explored four common strategies for sampling power injections for training neural networks that approximate voltage magnitudes. The paper also introduces a new sampling strategy that combines the four strategies into one dataset.

Extensive numerical results characterize how the NN prediction accuracy varies with the choice of training data sampling strategies. The results show that combining the four previously used data sampling strategies into one yields the best accuracy

TESTED WITH	TRAINED WITH: UNDERLOADING CS	CV	US	UV	Combined	NOMINAL LOADING CS	CV	US	UV	Combined	OVERLOADING CS	CV	US	UV	Combined	
CS	62.10	56.66	0.75	0.78	62.38	96.21	99.92	9.63	9.84	99.78	22.26	28.59	0.00	0.00	24.63	
CV	64.68	54.20	0.76	0.77	58.32	96.19	99.03	8.40	8.78	100.00	21.86	28.62	0.00	0.00	24.08	
US	53.24	48.04	0.00	0.00	58.21	95.58	100.00	24.46	29.06	100.00	21.42	27.51	0.00	0.00	23.43	ε = 0.001
UV	52.47	47.42	0.00	0.00	57.98	95.62	100.00	25.12	29.87	100.00	21.79	27.96	0.00	0.00	23.57	
Combined	57.74	51.88	0.18	0.19	59.25	95.92	99.66	17.28	19.95	99.85	21.72	27.78	0.00	0.00	23.82	
CS	62.10	56.66	0.75	0.78	62.38	96.21	99.92	9.63	9.84	99.41	22.26	28.59	0.00	0.00	24.63	
CV	64.68	54.20	0.76	0.77	58.32	96.19	99.03	8.40	8.78	99.78	21.86	28.62	0.00	0.00	24.08	
US	53.24	48.04	0.00	0.00	58.21	95.58	100.00	24.46	29.06	100.00	21.42	27.51	0.00	0.00	23.43	ε = 0.002
UV	52.47	47.42	0.00	0.00	57.98	95.62	100.00	25.12	29.87	100.00	21.79	27.96	0.00	0.00	23.57	
Combined	57.74	51.88	0.18	0.19	59.25	95.92	99.66	17.28	19.95	99.85	21.72	27.78	0.00	0.00	23.82	
CS	95.57	92.03	1.78	1.88	91.51	99.81	100.00	23.49	24.13	100.00	52.98	71.82	0.00	0.00	63.71	
CV	96.22	92.17	2.05	2.08	92.88	99.81	100.00	21.45	21.81	100.00	51.74	69.82	0.00	0.00	62.48	
US	98.05	92.90	0.00	0.00	93.01	99.77	100.00	52.93	59.31	100.00	50.31	70.30	0.00	0.00	62.59	ε = 0.005
UV	97.22	92.44	0.00	0.00	92.65	99.79	100.00	53.82	60.12	100.00	51.07	70.95	0.00	0.00	62.71	
Combined	96.88	92.32	0.43	0.47	92.34	99.79	100.00	38.80	42.38	100.00	51.30	70.77	0.00	0.00	62.53	
CS	100.00	99.95	3.35	3.63	99.89	100.00	100.00	43.94	44.45	100.00	94.69	92.71	0.00	0.00	92.99	
CV	100.00	99.99	4.36	4.57	99.96	100.00	100.00	43.60	43.96	100.00	94.25	92.25	0.00	0.00	92.52	
US	100.00	100.00	0.00	0.00	100.00	100.00	100.00	79.72	82.68	100.00	96.08	92.62	0.00	0.00	92.52	ε = 0.01
UV	100.00	100.00	0.00	0.00	100.00	100.00	100.00	80.23	83.06	100.00	96.77	92.36	0.00	0.00	92.85	
Combined	100.00	99.98	1.15	1.25	99.96	100.00	100.00	62.09	63.99	100.00	95.41	92.22	0.00	0.00	92.50	

(d) Swedish 503-bus system

TESTED WITH	TRAINED WITH: UNDERLOADING CS	CV	US	UV	Combined	NOMINAL LOADING CS	CV	US	UV	Combined	OVERLOADING CS	CV	US	UV	Combined	
CS	69.10	61.58	43.80	49.69	96.43	100.00	99.89	100.00	100.00	100.00	17.59	27.61	6.15	5.21	33.40	
CV	70.03	62.61	45.20	50.98	96.56	100.00	99.89	100.00	100.00	100.00	16.99	26.51	6.08	5.08	32.47	
US	79.56	59.94	29.30	40.42	99.59	100.00	99.89	100.00	100.00	100.00	14.94	28.58	5.86	5.30	29.48	ε = 0.001
UV	79.22	59.30	27.52	39.29	99.49	100.00	99.89	100.00	100.00	100.00	14.82	28.89	5.86	5.33	29.46	
Combined	75.61	61.50	36.70	45.45	98.25	100.00	99.89	100.00	100.00	100.00	16.30	27.91	6.00	5.25	31.48	
CS	69.10	61.58	43.80	49.69	96.43	100.00	99.89	100.00	100.00	100.00	17.59	27.61	6.15	5.21	33.40	
CV	70.03	62.61	45.20	50.98	96.56	100.00	99.89	100.00	100.00	100.00	16.99	26.51	6.08	5.08	32.47	
US	79.56	59.94	29.30	40.42	99.59	100.00	99.89	100.00	100.00	100.00	14.94	28.58	5.86	5.30	29.48	ε = 0.002
UV	79.22	59.30	27.52	39.29	99.49	100.00	99.89	100.00	100.00	100.00	14.82	28.89	5.86	5.33	29.46	
Combined	75.61	61.50	36.70	45.45	98.25	100.00	99.89	100.00	100.00	100.00	16.30	27.91	6.00	5.25	31.48	
CS	99.99	99.92	95.18	97.09	100.00	100.00	100.00	100.00	100.00	100.00	78.44	91.64	31.89	29.47	98.07	
CV	99.96	99.90	95.26	97.25	100.00	100.00	100.00	100.00	100.00	100.00	76.05	91.33	29.19	27.29	97.78	
US	100.00	100.00	99.89	99.99	100.00	100.00	100.00	100.00	100.00	100.00	83.38	93.45	26.59	24.47	99.63	ε = 0.005
UV	100.00	100.00	99.83	100.00	100.00	100.00	100.00	100.00	100.00	100.00	83.29	93.63	26.88	24.34	99.72	
Combined	99.99	99.94	97.87	98.79	100.00	100.00	100.00	100.00	100.00	100.00	80.52	92.90	29.04	26.76	98.81	
CS	100.00	100.00	100.00	100.00	100.00	100.00	100.00	100.00	100.00	100.00	100.00	100.00	98.88	98.32	100.00	
CV	100.00	100.00	100.00	100.00	100.00	100.00	100.00	100.00	100.00	100.00	100.00	100.00	98.89	98.31	100.00	
US	100.00	100.00	100.00	100.00	100.00	100.00	100.00	100.00	100.00	100.00	100.00	100.00	100.00	99.99	100.00	ε = 0.01
UV	100.00	100.00	100.00	100.00	100.00	100.00	100.00	100.00	100.00	100.00	100.00	100.00	100.00	99.98	100.00	
Combined	100.00	100.00	100.00	100.00	100.00	100.00	100.00	100.00	100.00	100.00	100.00	100.00	99.46	99.21	100.00	

(e) European 906-bus system

Fig. 2: Heatmaps of the PTol metric for different tolerance levels, $\epsilon = 0.01, 0.005, 0.002, 0.001$ across different datasets. Darker colors represent higher values of PTol and indicate better approximation accuracy. The columns indicate the training set, and the rows indicate the test set. Results along the main diagonal of the table show approximation accuracy when the neural network is trained and tested on the same dataset. Off-diagonal entries correspond to testing on datasets that use different sampling strategies than used during training to assess generalizability.

and least spread in error. This combined strategy outperformed the other four strategies in both nominal and extreme loading conditions. When tested with time series data, the combined strategy again produced a minimal approximation error compared to each other strategy individually.

Future work will investigate the best sampling methods for other applications in power systems beyond voltage magnitude predictions, including optimal power flow and unit commitment problems.

REFERENCES

[1] B. K. Bose, "Artificial Intelligence Techniques in Smart Grid and Renewable Energy Systems—Some Example Applications," *Proceedings of the IEEE*, vol. 105, pp. 2262–2273, Nov. 2017.

[2] M. Khodayar, G. Liu, J. Wang, and M. E. Khodayar, "Deep learning in power systems research: A review," *CSEE Journal of Power and Energy Systems*, vol. 7, pp. 209–220, Mar. 2021.

[3] J. Xie, I. Alvarez-Fernandez, and W. Sun, "A Review of Machine Learning Applications in Power System Resilience," in *IEEE Power & Energy Society General Meeting (PESGM)*, Aug. 2020.

[4] W. Shi, X. Han, X. Wang, S. Gu, and Y. Hao, "Application of Artificial Intelligence and Its Interpretability Analysis in Power Grid Dispatch and Control," in *8th Asia Conference on Power and Electrical Engineering (ACPEE)*, pp. 1704–1711, Apr. 2023.

[5] K. D. Tuan, T. L. B. Duy, and H. L. Van, "Applying Artificial Intelligence To Distribution Network State Estimation," in *International Symposium on Electrical and Electronics Engineering (ISEE)*, pp. 179–184, Oct. 2023.

[6] S. Jie, Z. Yanxia, W. Xiong, and N. Xueying, "Exploration on Artificial Intelligence Technology in Power System State Estimation, Monitoring and Early Warning System," in *IEEE 3rd International Conference on Data Science and Computer Application (ICDSCA)*, pp. 1423–1429, Oct. 2023.

[7] A. Almalaq and G. Edwards, "A Review of Deep Learning Methods Applied on Load Forecasting," in *16th IEEE International Conference on Machine Learning and Applications (ICMLA)*, pp. 511–516, Dec. 2017.

[8] J. Duan, D. Shi, R. Diao, H. Li, Z. Wang, B. Zhang, D. Bian, and Z. Yi, "Deep-Reinforcement-Learning-Based Autonomous Voltage Control for Power Grid Operations," *IEEE Transactions on Power Systems*, vol. 35, pp. 814–817, Jan. 2020.

[9] H. Salazar, R. Gallego, and R. Romero, "Artificial Neural Networks and Clustering Techniques applied in the Reconfiguration of Distribution systems," *IEEE Transactions on Power Delivery*, vol. 21, pp. 1735–1742,

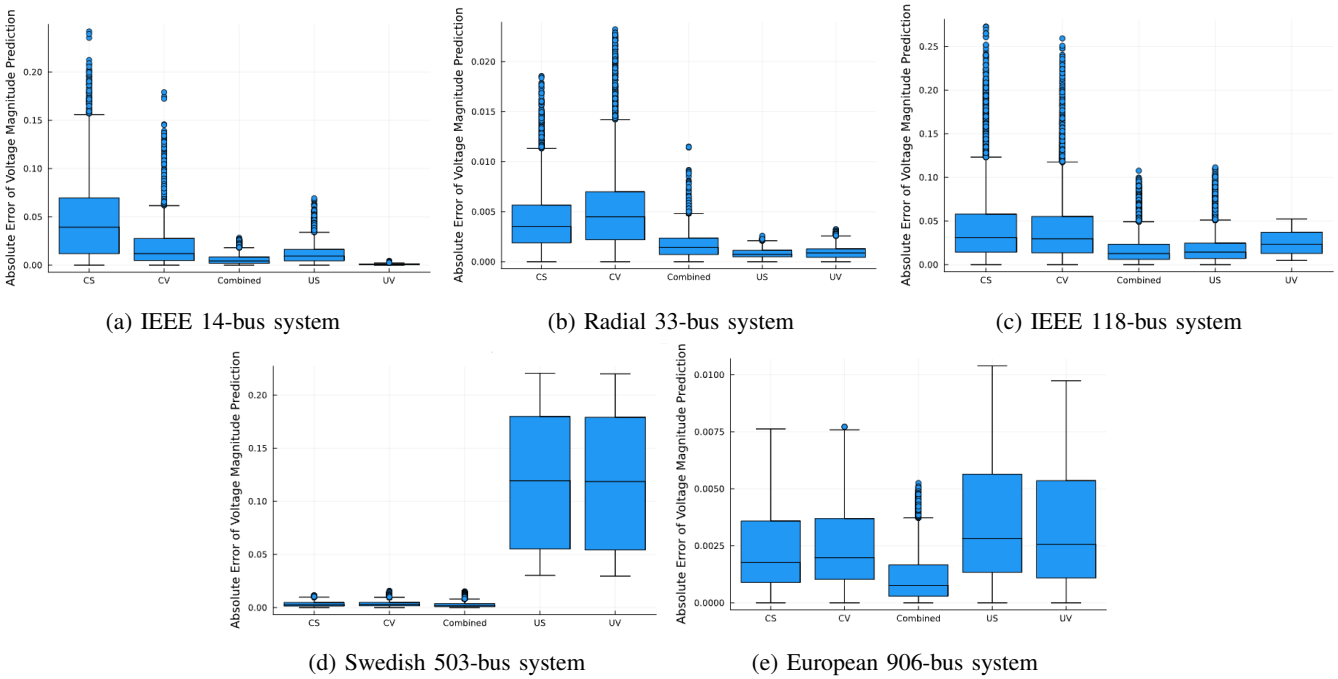

(a) IEEE 14-bus system (b) Radial 33-bus system (c) IEEE 118-bus system

(d) Swedish 503-bus system (e) European 906-bus system

Fig. 3: Boxplots showing the spread of voltage prediction errors of different methods when tested with the time series data.

July 2006.

[10] R. Haider and A. M. Annaswamy, "Grid-SiPhyR: An end-to-end Learning to Optimize framework for Combinatorial problems in Power Systems," May 2023. arXiv:2206.06789 [cs, eess].

[11] A. S. Zamzam and K. Baker, "Learning Optimal Solutions for Extremely Fast AC Optimal Power Flow," in *IEEE International Conference on Communications, Control, and Computing Technologies for Smart Grids (SmartGridComm)*, Nov. 2020.

[12] H. Akhavan-Hejazi and H. Mohsenian-Rad, "Power Systems Big Data Analytics: An Assessment of Paradigm Shift Barriers and Prospects," *Energy Reports*, vol. 4, pp. 91–100, Nov. 2018.

[13] Q. Yang *et al.*, "Two-Timescale Voltage Control in Distribution Grids Using Deep Reinforcement Learning," *IEEE Trans. Smart Grid*, vol. 11, no. 3, pp. 2313–2323, 2020.

[14] R. Henry and R. K. Gupta, "Measurement-based/Model-less Estimation of Voltage Sensitivity Coefficients by Feedforward and LSTM Neural Networks in Power Distribution Grids," in *IEEE TPEC*, 2024.

[15] J. Kotary, F. Fioretto, and P. Van Hentenryck, "Learning Hard Optimization Problems: A Data Generation Perspective," in *Advances in Neural Information Processing Systems*, vol. 34, pp. 24981–24992, 2021.

[16] K. Baker, "Learning Warm-Start Points For AC Optimal Power Flow," in *IEEE 29th International Workshop on Machine Learning for Signal Processing (MLSP)*, 2019.

[17] S. Misra, L. Roald, and Y. Ng, "Learning for Constrained Optimization: Identifying Optimal Active Constraint Sets," *INFORMS Journal on Computing*, vol. 34, pp. 463–480, Jan. 2022.

[18] X. Pan, T. Zhao, and M. Chen, "DeepOPF: Deep Neural Network for DC Optimal Power Flow," in *IEEE International Conference on Communications, Control, and Computing Technologies for Smart Grids (SmartGridComm)*, Oct. 2019.

[19] D. Deka and S. Misra, "Learning for DC-OPF: Classifying active sets using neural nets," in *2019 IEEE Milan PowerTech*, pp. 1–6, 2019.

[20] J. Authier, R. Haider, A. Annaswamy, and F. Dörfler, "Physics-informed Graph Neural Network for Dynamic Reconfiguration of Power Systems," *Electric Power Systems Research*, vol. 235, p. 110817, Oct. 2024.

[21] N. Guha, Z. Wang, M. Wytock, and A. Majumdar, "Machine Learning for AC Optimal Power Flow," in *Climate Change Workshop at the International Conference on Machine Learning (ICML)*, June 2019.

[22] T. Pham and X. Li, "Neural Network-based Power Flow Model," in *IEEE Green Technologies Conference (GreenTech)*, pp. 105–109, Mar. 2022.

[23] M. Tuo, X. Li, and T. Zhao, "Graph Neural Network-Based Power Flow Model," in *North American Power Symposium (NAPS)*, Oct. 2023.

[24] D. P. Kingma and J. Ba, "Adam: A Method for Stochastic Optimization," *arXiv:1412.6980*, 2014.

[25] R. Gupta, F. Sossan, and M. Paolone, "Grid-aware Distributed Model Predictive Control of Heterogeneous Resources in a Distribution Network: Theory and Experimental Validation," *IEEE Transactions on Energy Conversion*, vol. 36, no. 2, pp. 1392–1402, 2020.

[26] R. Tabors, "A Wake-Up Call for the Utility Industry: Extreme Weather and Fundamental Lessons from 2021," *56th Hawaii International Conference on System Sciences (HICSS)*, Jan. 2023.

[27] H. Yuanyuan, J. Fei, L. Lizhou, H. Junyang, X. Ning, and L. Yetian, "Power Grid Load Analysis under Extreme Weather –Taking Tianfu New Area in Sichuan Province as an Example," in *Panda Forum on Power and Energy (PandaFPE)*, pp. 2096–2101, Apr. 2023.

[28] Y. Lv, B. Sun, M. Wang, Y. Jiao, X. Song, Y. Luo, and P. Lu, "Review on Modeling of Impact of Extreme Weather on Source-Grid-Load-Storage," in *IEEE 7th Conference on Energy Internet and Energy System Integration (EI2)*, pp. 1840–1845, Dec. 2023.

[29] M. Baran and F. Wu, "Network Reconfiguration in Distribution Systems for Loss Reduction and Load Balancing," *IEEE Transactions on Power Delivery*, vol. 4, no. 2, pp. 1401–1407, 1989.

[30] IEEE PES PGLib-OPF Task Force, "The Power Grid Library for Benchmarking AC Optimal Power Flow Algorithms," Jan. 2021. arXiv:1908.02788 [math].

[31] L. Thurner *et al.*, "Pandapower – An Open Source Python Tool for Convenient Modeling, Analysis and Optimization of Electric Power Systems," *IEEE Trans. Power Sys.*, vol. 33, no. 6, pp. 6510–6521, 2018.

[32] J. Bezanson, A. Edelman, S. Karpinski, and V. B. Shah, "Julia: A Fresh Approach to Numerical Computing," *SIAM Review*, vol. 59, pp. 65–98, Jan. 2017.

[33] C. Coffrin, R. Bent, K. Sundar, Y. Ng, and M. Lubin, "PowerModels. JL: An Open-Source Framework for Exploring Power Flow Formulations," in *Power Systems Computation Conference (PSCC)*, June 2018.

[34] A. Wächter and L. T. Biegler, "On the Implementation of an Interior-point filter Line-search Algorithm for Large-scale Nonlinear Programming," *Mathematical Programming*, vol. 106, pp. 25–57, Mar. 2006.

[35] M. Innes, "Flux: Elegant Machine Learning with Julia," *Journal of Open Source Software*, vol. 3, p. 602, 2018.